Journal of Physics: Conference Series **441** (2013) 012034 doi:10.1088/1742-6596/441/1/012034

# Fabrication of iron oxide nanoparticles using laser ablation in liquids

**T Iwamoto[1] and T Ishigaki[2]**

[1]Institute of Sustainability Research and Education, Hosei University, 2-17-1 Fujimi, Chiyoda-ku, Tokyo 102-8160, Japan

[2]Department of Chemical Science and Technology, Hosei University, 3-7-2 Kajino-cho, Koganei-shi, Tokyo 184-8584, Japan

E-mail: ishigaki@hosei.ac.jp

**Abstract**. Nanoparticles of iron oxides were synthesized through the ablation of the bulk-targets of Fe, $Fe_3O_4$, and $Fe_2O_3$ in water by the irradiation of a Nd:YAG laser. Our samples prepared via the laser ablation method displayed small (ca. 1 nm in diameter) and large (over 5 nm in diameter) particles. The small particles were well-dispersed, whereas large particles were agglomerated. The FeO and $Fe_3O_4$ phases were formed in the synthesized powders irrespective of the kind of targets. The formation of the other phases, Fe and $Fe_2O_3$, changed depending on the the kind of targets used in the laser ablation. Poly(*N*-vinyl-2-pyrrolidone) (PVP) as a protective reagent was employed to disperse large particles in our samples, and accordingly, their dispersibility was improved as mole concentration of PVP increased.

## 1. Introduction

Iron oxide is known broadly as a magnetic material such as a permanent magnet. In iron oxide, three kinds of FeO, $Fe_3O_4$, and $Fe_2O_3$ exist and each is applied in different fields. Recently, iron oxide nanoparticles have been synthesized by various routes, and their crystal structure and magnetic property have been investigated in detail [1–7]. At present, new applications like hyperthermia and a drug delivery system using iron oxide nanoparticles are also expected, to say nothing of ordinary applications of pigment, contrast medium, and magnetic devices using iron oxide in a bulk state.

In general, chemical and physical routes have been chosen as syntheses of nanoparticles. The main advantage of chemical routes is to yield a large amount of nanoparticles, while that of physical routes is to fabricate nanoparticles with high-crystallinity. Recently, a laser ablation method in physical routes has been focused on, especially since it is easy and eco-friendly and possesses only a few experimental parameters [8–13]. Moreover, this method can provide free-standing nanoparticles, and hence their intrinsic properties can be examined because nanoparticles prepared by chemical methods are usually protected by organic molecules. However, nanoparticles synthesized by the laser ablation method are often agglomerated, and thus there is an unsolved problem with respect to nanomaterials prepared by this method [8–13].

In the present paper, iron oxide nanoparticles are fabricated via the laser ablation method, and their morphology and crystal structure are investigated. Additionally, to disperse the iron oxide nanoparticles prepared using the laser ablation method, we employ organic molecules as a protective reagent and examine their effect on dispersibility and the crystal structure of the nanoparticles.

## 2. Experimental procedure

To ablate three kinds of targets (Fe, $Fe_2O_3$, and $Fe_3O_4$, purity 99.99%, Kojundo Chemical Laboratory Co., Ltd., Saitama, Japan) and synthesize nanoparticles, a Nd:YAG laser (Quantel Brilliant b, Les Ulis, France) with pulse duration of 6 ns, a wavelength of 1064 nm and a repetition rate of 10 Hz was used [14,15]. Figure 1 schematically illustrates the experimental setup. The target was fixed on the bottom of a glass beaker (20 ml), and distilled water as a solvent was added at a level of 10 mm from the target-surface. The beaker was rotated at 40 rpm and target-surface was irradiated for 1 h by the Nd:YAG laser with a laser spot of approximately 250 μm. Then, colloidal nanoparticles were collected.

Crystal structure of nanoparticles was estimated by using X-ray diffraction (XRD, Rigaku SmartLab, 40 kV, 30 mA, CuKa 0.1541 nm, Tokyo, Japan). Morphology and dispersibility of nanoparticles were investigated by transmission electron microscopy (TEM, JEOL JEM-2100F, Tokyo, Japan).

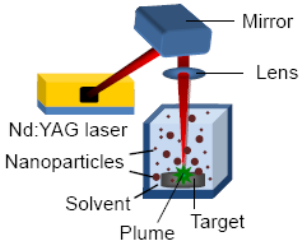


**Figure 1.** Schematic illustration of experimental setup.

## 3. Results and discussion

Figures 2(a) and 2(b) show TEM photographs of our sample prepared at laser power of 100 mW for 1 h by using a Fe target. Small particles and large particles co-exist. Figure 2(c) displays a size distribution histogram of small particles seen in Fig. 2(a). The particles exhibit a mean diameter of 1.0 nm and a standard deviation of 0.1 nm. The small particles are highly dispersed, but large particles over 5 nm in diameter are agglomerated. These mono- and highly-dispersed small nanoparticles in the case of the laser ablation method do not appear in the previous literatures on agglomerated iron oxide nanoparticles with 10-50 nm in diameter [8,10,13]. In Fig. 1(d), an XRD pattern of the sample exhibits Fe, FeO, and $Fe_3O_4$ peaks. $Fe_3O_4$ is the main product because this pattern corresponds to bulk-$Fe_3O_4$ profile. Hence, this sample is a mixture of iron and iron oxide.

Figure 3 provides XRD patterns of our samples synthesized at various laser powers for 1 h by using Fe, $Fe_2O_3$, and $Fe_3O_4$ targets. In the case of a Fe target, Fe, FeO, and $Fe_3O_4$ peaks are detected. $Fe_2O_3$ peaks are also detected as laser power increases. When a $Fe_2O_3$ target is used, FeO, $Fe_2O_3$, and $Fe_3O_4$ peaks are seen and, FeO and $Fe_2O_3$ peaks increase as laser power increases. When a $Fe_3O_4$ target is used, FeO and $Fe_3O_4$ peaks are detected and FeO is decreased by increasing laser power. However, the $Fe_2O_3$ peak at 33° is detected as laser power increases like in the case of the Fe target. This probably suggests that FeO is oxidized to $Fe_2O_3$ because temperature and pressure in the plume seen in Fig. 1 increase as laser power increases. Moreover, the kind of targets may influence initial particles evaporated from these targets. In all targets, FeO and $Fe_3O_4$ peaks are detected in our samples. S.-Warkocka et al. claimed that $Fe_3O_4$ nanoparticles were reduced to form FeO phase [12].

$Fe_3O_4$ is the main product in our samples, and $Fe_3O_4$ diffractions are seen together with other iron oxide ones similar to those in the case of our samples also in Ref. [9,11,12]. Here, we consider the relationship between temperature and $O_2$ partial pressure in the iron oxide phase, which is determined by the $H_2/H_2O$ equilibrium in the plume at high temperature. In the light of an Ellingham diagram [16], which represents many oxides in thermodynamic states and determines their $O_2$ partial pressure, our experimental environment probably keeps the most proper balance between temperature and $O_2$ partial pressure. When target and laser power are altered, a balance of the $O_2$ partial pressure in the plume is broken by ablating the target and generating new O atoms, the $O_2$ partial pressure in the plume changes, and then other iron oxides (FeO or $Fe_2O_3$) are prepared.

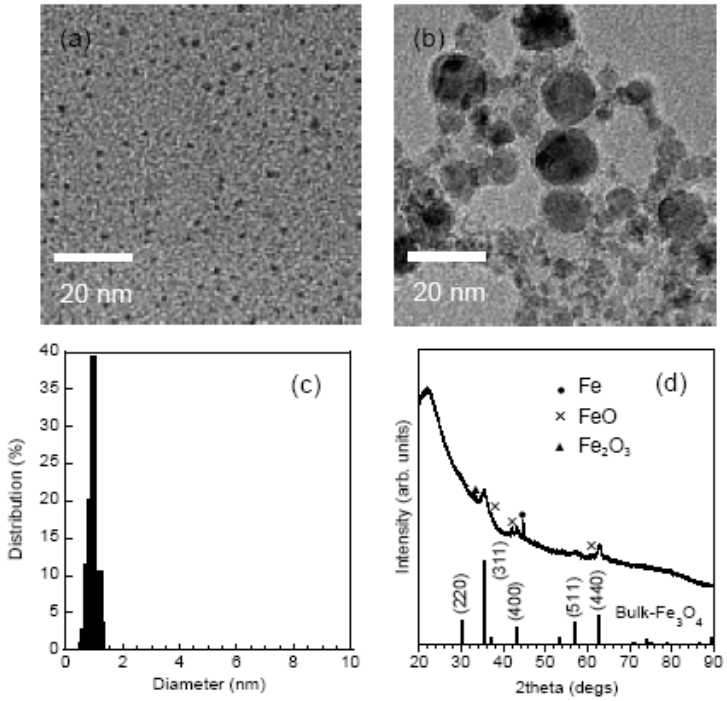


**Figure 2.** TEM photographs of (a) small and (b) large nanoparticles in our sample prepared at laser power of 100 mW for 1 h using a Fe target. (c) A size distribution histogram of (a). A mean diameter is 1.0 nm and standard deviation is 0.1 nm. (d) An XRD pattern of the sample. The bulk-$Fe_3O_4$ profile is taken from ICDD, No. 01-089-2355. The values in the graph represent the index of plane for $Fe_3O_4$.

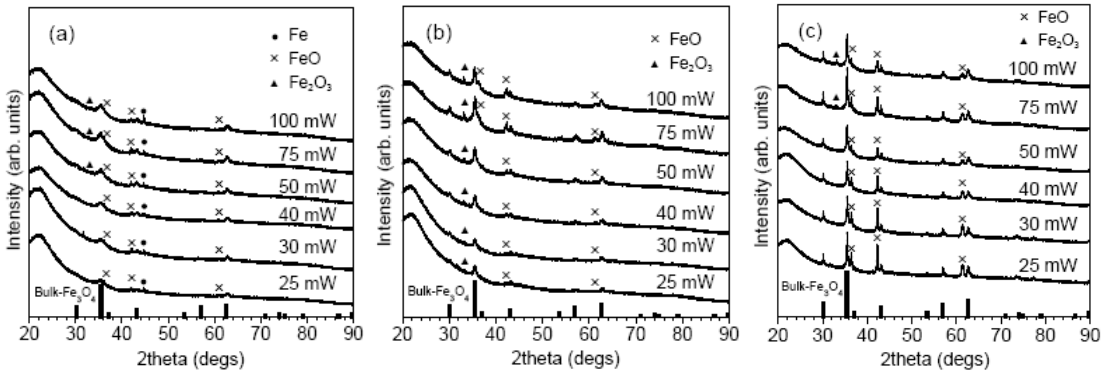


**Figure 3.** XRD patterns of samples synthesized at various laser powers for 1 h by using (a) Fe, (b) $Fe_2O_3$, and (c) $Fe_3O_4$ targets. The bulk-$Fe_3O_4$ profile is taken from ICDD, No. 01-089-2355.

As shown in Figs. 2(a) and 2(b), small particles are dispersed, whereas large particles are agglomerated. Yang explained the evolution of the laser-induced plasma in liquid and reported that four kinds of chemical reactions occurred inside the plasma and liquid, and the interface between the plasma and liquid [17]. Since the first chemical reaction occurs inside the laser-induced plasma, the small initial particles are synthesized as shown in Fig. 2(a). After that, the second chemical reaction also takes place inside the plasma. However, some initial particles escape from the plume and enter the liquid area, where cooling takes place and further grain growth stops. In the second chemical reaction, the other initial particles remaining in the plasma grow into large particles at high temperature. Therefore, small and large particles exist in our samples.

To avoid the formation of large particles, organic molecules were used as a protective reagent. We tried to synthesize iron oxide nanoparticles by using various organic molecules such as several kinds of amino acids and sodium dodecyl sulfate, and consequently, it was found that poly(*N*-vinyl-2-pyrrolidone) (PVP, an average molecular weight of 55,000, Sigma-Aldrich), which was very useful in chemical syntheses of metallic alloy nanoparticles [18–20], was the best protective reagent in our experiments. Herein, we prepare iron oxide nanoparticles via the laser ablation in water containing PVP by using a $Fe_3O_4$ target. Figure 4 presents TEM photographs of samples prepared at laser power of 50 mW for 1 h under various mole concentrations of PVP. As PVP concentration increases, large particles are dispersed. Small particles around 1.0 nm in diameter show high-dispersibility as seen in Fig. 2(a) irrespective of PVP concentration (not shown).

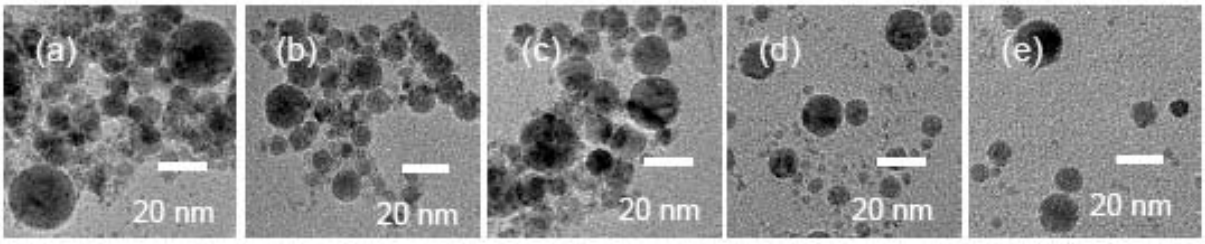


**Figure 4.** TEM photographs of large particles in samples prepared at laser power of 50 mW for 1 h under various mole concentrations of PVP by using a $Fe_3O_4$ target.: (a) without PVP and (b) 0.01, (c) 5, (d) 20, and (e) 50 mM of PVP.

Figure 5 exhibits XRD patterns of samples fabricated at laser power of 50 mW for 1 h and various mole concentrations of PVP by using a $Fe_3O_4$ target. When PVP concentration increases, these diffractions are broad, and hence, crystalline sizes of samples coated by PVP become small. This result has been reported in the previous literature with respect to PVP-coated FePt nanoparticles prepared by chemical routes [20]. By increasing the amount of PVP, the growth of nanoparticles may be retarded due to coating them with a large amount of PVP. PVP as a protective reagent affects dispersibility and crystalline size of nanoparticles irrespective of the kind of syntheses (chemical or physical methods).

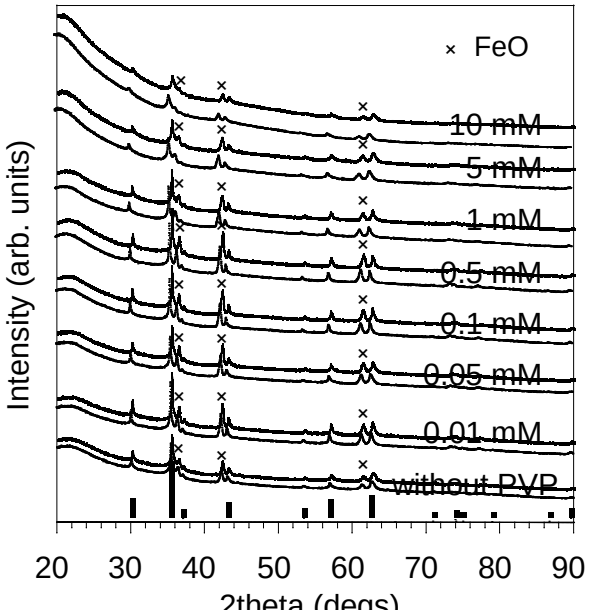


**Figure 5.** XRD patterns of samples prepared at laser power of 50 mW for 1 h under various concentrations of PVP by using a $Fe_3O_4$ target. The bulk-$Fe_3O_4$ profile is taken from ICDD, No. 01-089-2355.

## 4. Conclusion

In conclusion, the present paper provided some new information. Our samples prepared via the laser ablation method showed small (ca. 1 nm in diameter) and large (over 5 nm in diameter) particles. Targets used in the laser ablation affected crystal structure of our samples. Irrespective of targets, FeO and $Fe_3O_4$ peaks were detected. When PVP was used as a protective reagent to disperse large particles, their dispersibility was improved as mole concentration of PVP increased. By adding PVP, crystalline sizes became small.

## Acknowledgment

We thank Mr. M. Ichihara at Precision Analysis Laboratory, Hosei University, for his assistance in TEM observations.

## References

[1] Pérez J A L, Quintela M A L, Mira J, Rivas J and Charles S W 1997 *J. Phys. Chem. B* **101** 8045
[2] Morales M P, Veintemillas-Verdaguer S, Montero M I, Serna C, Roig A, Casas L, Martínez B and Sandiumenge F 1999 *Chem. Mater.* **11** 2058
[3] Sun S and Zeng H 2002 *J. Am. Chem. Soc.* **124** 8204
[4] Teng X and Yang H 2004 *J. Mater. Chem.* **14** 774
[5] Pinna N, Grancharov S, Beato P, Bonville P, Antonietti M and Niederberger M 2005 *Chem. Mater.* **17** 3044
[6] Cai W and Wan J 2007 *J. Colloid Interface Sci.* **305** 366
[7] Laurent S, Forge D, Port M, Roch A, Robic C, Elst L V and Muller R N 2008 *Chem. Rev.* **108** 2064
[8] Zeng X, Wang Z, Liu Y and Ji M 2005 *Appl. Phys. A* **80** 581
[9] Kurland H-D, Grabow J, Staupendahl G, Andrä W, Dutz S and Bellemann M E 2007 *J. Magn. Magn. Mater.* **311** 73
[10] Liu P, Cai W and Zeng H 2008 *J. Phys. Chem. C* **112** 3261
[11] Amendola V, Riello P and Meneghetti M 2011 *J. Phys. Chem. C* **115** 5140
[12] Swiatkowska-Warkocha Z, Kawaguchi K, Wang H, Katou Y and Koshizaki N 2011 *Nanoscale Res. Lett.* **6** 226
[13] Osipov V V, Platonov V V, Uimin M A and Podkin A V 2012 *Tech. Phys.* **57** 543
[14] Al-Mamun S A, Nakajima R and Ishigaki T 2012 *Thin Solid Films* **523** 46
[15] Al-Mamun S A, Nakajima R and Ishigaki T 2013 *J. Colloid Interface Sci.* **392** 172
[16] Ellingham H J T 1944 *J. Soc. Chem. Ind., London* **63** 125
[17] Yang G W 2007 *Prog. Mater. Sci.* **52** 648
[18] Iwamoto T, Matsumoto K, Kitamoto Y and Toshima N 2007 *J. Colloid Interface Sci.* **308** 564
[19] Iwamoto T, Kitamoto Y and Toshima N 2009 *Physica B* **404** 2080
[20] Iwamoto T, Matsumoto K, Matsushita T, Inokuchi M and Toshima N 2009 *J. Colloid Interface Sci.* **336** 879